

Communication-Constrained Routing and Traffic Control for Autonomous Vehicles

Guangyi Liu, *Student Member, IEEE*, Seyedmohammad Salehi, *Student Member, IEEE*, Erdem Bala, *Member, IEEE*, Chien-Chung Shen, *Member, IEEE*, and Leonard J. Cimini, *Fellow, IEEE*

Abstract—Autonomous vehicles (AV) is an advanced technology that can bring convenience, improve the road-network throughput, and reduce traffic accidents. To enable higher levels of automation (LoA), massive amounts of sensory data need to be uploaded to the network for processing, and then, maneuvering decisions must be returned to the AV. Furthermore, passengers might have a higher transmission rate demands for various data hungry and delay-sensitive applications. However, due to frequent channel variations and imperfect cell deployments, guaranteeing a minimum transmission rate is impossible during a trip. In this work, the communication constraints of AVs are discussed. With these constraints, we present high-level concepts for the communication-constrained routing and traffic control optimization problems. First, to satisfy the minimum transmission rate requirements for the AV's LoA and certain applications used in the vehicle, we propose to divide the road network into two layers and perform a two-layered routing scheme; compared to some greedy methods, this scheme achieves a better balance between trip duration and communication coverage. Furthermore, for optimal traffic control purposes, we propose a key performance index (KPI) to evaluate the traffic control capability of cellular systems. Then, two lemmas are proposed and proved to guide the goal of achieving optimal traffic flow with constrained communication resources.

Index Terms—autonomous vehicles, routing, communication-constrained, traffic control, road-network throughput

I. INTRODUCTION

The technology of autonomous vehicles (AVs) has the potential to drastically reduce the energy consumption, traffic congestion, and collisions of vehicles [1], [2]. In [3], five levels of automation (LoA) of AVs are described: (0) no automation, (1) driver assistance, (2) partial automation, (3) conditional automation, (4) high automation, and (5) full automation. With different LoA, AVs can enable new applications, such as dynamic ridesharing, platooning, remote driving, to name a few [3]. To achieve a higher LoA, AVs need to, throughout the entire trip, constantly communicate with neighboring AVs, as well as with traffic control services running in the infrastructure that continuously monitor the status of each AV and its surrounding environment to make driving decisions. Specifically, because AVs might not have sufficient computing capacity for machine or deep learning based video/data processing, it has been proposed that portions of the data processing and driving decisions be delegated to the edge or to the cloud [3], [24]. Therefore, the availability, reliability, latency, and sustainable transmission rate of AV's connectivity with traffic control services running in the infrastructure are

critical to achieve a high LoA [3]–[6]. However, with AV's high mobility and the associated dynamic environment, these communication requirements bring significant challenges to the cellular infrastructure [7]–[9].

To provide wireless connectivity with higher quality-of-service (QoS) and reliability, fifth generation cellular systems (5G) will support use cases such as enhanced mobile broadband (eMBB), massive machine type communications (mMTC), and ultra-reliable low-latency communications (URLLC) for mission-critical applications [7], [11]. To enable these use cases, disruptive technologies, such as massive multiple-input and multiple-output (MIMO) and millimeter wave (mmWave), are expected to be deployed [7]. In [14], it is shown that four out of the nine 5G deployment scenarios support vehicular communication. These are 1) Broadband Access in Dense Areas - providing 300 Mbps for vehicles with speeds up to 60 mph; 2) 50+ Mbps Everywhere - providing 50 Mbps with speeds up to 60 mph; 3) Mobile Broadband in Vehicles - providing 50 Mbps with speeds up to 300 mph; and 4) Ultra-Low Cost Broadband Access for Low Average Revenue Per User (ARPU) Areas - providing 10 Mbps with speeds up to 30 mph. The actual deployment of 5G is likely to support a mixture of these scenarios across all regions.

Among the LoA, high and full automation would heavily rely on constant communication between an AV and the back-end services running in the infrastructure. Typically, 50+ Mbps high-reliability low-latency communications is required during the entire trip to facilitate higher LoA and to accommodate any higher data rates demanded by passenger applications [3]. However, even when 5G is fully deployed, among the nine 5G deployment scenarios, only the “Broadband Access in Dense Areas” use case can guarantee the sum transmission rate requirement imposed by the LoA of high and full automation. In addition, it could take several years to cover all the major areas with 5G, and the quality of communication is often worse around the cell boundaries. Therefore, without proper route planning, there is no guarantee that the sum-rate requirement imposed by the high LoA of the AVs can be sustained during the entire trip, especially when the density of AVs is high along certain road paths.

In order to facilitate high LoA for the AVs during the entire ride, here, we propose a communication-constrained routing (CCR) problem, where, given the finite and different amounts of communication resources along the different road segments (RSs) and intersections (RIs), the routes of AVs are deliberately selected, such that the minimum sum transmission rate requirements of the AVs can be satisfied at all times. In addition, we also propose a communication-constrained traffic

G. Liu, S. Salehi, C.-C. Shen, and L. J. Cimini are with the University of Delaware, Newark, DE (e-mail: guangyi, salehi, cshen, cimini@udel.edu). E. Bala is with InterDigital (e-mail: Erdem.Bala@interdigital.com).

control (CCTC) problem, where the communication resources available over different roads can be utilized to maximize road-network throughput. To the best of our knowledge, CCR and CCTC are new classes of routing and resource allocation problems, respectively, that have not yet been explored. Only a recent 3GPP document [3] elaborating the QoS aspects of automated driving (Section 5.27.2.1) and remote driving (Section 5.28.2.2) describe selecting routes that can support the required communication QoS.

Previous work related to this topic includes energy-constrained routing and traffic optimization problems discussed in the context of electric vehicles [15]–[17]. However, the graph-based models adopted for road networks in electric vehicle routing cannot be properly adapted to either CCR or CCTC. The difficulties can be attributed to the fact that (1) there are no detailed models connecting the key performance indexes (KPIs) of wireless communication with those of AV movement; and (2) the edge weights of any routing graph computed from the sum transmission rates of wireless communication may not be stable due to the fast time-varying nature of wireless channels. These two technical issues will be specifically addressed in this paper.

From the aspect of shortest path routing, one major challenge is to reduce the time complexity for large networks [10], [15], [18]–[20]. In practice, a subset of critical nodes are often selected to divide the network into multiple layers, such that hierarchical routing can be applied with some preprocessing [2], [18]–[20]. However, the performance of hierarchical routing is strongly dependent on the selection of these critical nodes, which is often suboptimal. For CCR in large road networks, computing the theoretical minimum-trip-time route is a critical issue that is also addressed in this paper.

In terms of resource allocation, traffic control for AVs is an important issue that has been studied [21], [22]. Without taking the communication constraints into consideration, backpressure-based traffic control, which maximizes the road-network throughput, is proposed in [21]. However, coupled with the CCR problem, when the density of AVs is high, the limited communication resources may not be able to satisfy the communication needs of all AVs. Under this constraint, we also study how to optimally utilize the available resources to maximize the road-network throughput.

In this paper, we first describe an approach to modeling both the communication constraints for AVs and their effects on providing reliable wireless connectivity for higher LoA and reliable control. Then, by focusing on one individual AV, and without considering the impacts from other AVs, a non-convex optimization problem is formulated to minimize that AV’s trip duration, subject to a transmission rate requirement. For faster routing computation in large road networks, a new hierarchical routing scheme is proposed, which divides the computed routing graph into a top layer containing all the base stations (BSs) and a bottom layer containing local graphs made up of RIs and RSs. The optimality of this hierarchical scheme is demonstrated. In addition, simulation results show that, compared with certain greedy algorithms, this two-layered routing scheme provides longer communication coverage durations and acceptable source-to-destination trip duration.

For optimal traffic control, we focus on maximizing the road-network throughput subject to a constraint on the communication resources within a certain area. This is due to the fact that the complexity of performing city-wide, joint traffic control and route planning of all AVs is high. Therefore, we allow AVs to be navigated in a non-cooperative manner and focus on improving the road-network throughput for a given area. Specifically, to characterize the traffic control performance of wireless communication for AV traffic control, we propose and investigate a new KPI for traffic control in cellular systems. Using this KPI, two lemmas are proved to determine the optimal speed of each AV and optimal frequency channel allocation across multiple cells. Numerical results are provided to show the performance gain.

The rest of the paper is organized as follows. In Section II, the impacts of communication on AV routing and traffic control are discussed, motivating the introduction of two concepts to facilitate the study of CCR and CCTC. Section III studies the CCR problem, where a road network is modeled as a two-layer graph to facilitate a two-layered communication-constrained routing scheme. Simulation results are presented to demonstrate the effectiveness of the proposed scheme. Section IV investigates the CCTC problem by first computing AV speed within a single cell to maximize road-network throughput. Then, to match traffic flow across adjacent cells, a spectrum re-balancing solution is introduced to maximize AV road-network throughput across multiple cells. The effectiveness of the solution is validated via numerical studies. Section V concludes the paper and suggests future research directions.

II. IMPACTS OF COMMUNICATION ON ROUTING AND TRAFFIC CONTROL AVS

This section discusses the impacts of communication on the routing and traffic control of AVs, and introduces *effective speed map* (ESM) and γ -rate cell of a BS.

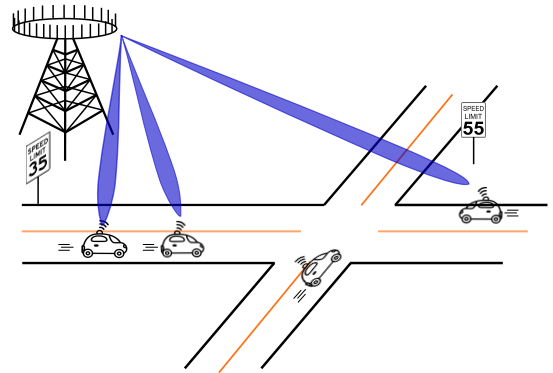


Figure 1: Infrastructure to AV communication

A. Effective Speed Map (ESM)

The speed of the AVs is a critical parameter for both routing and traffic control. For routing, given the distance of a road path between the source and destination, the speed determines the driving time for an AV to complete its route. For traffic

control, the throughput of the road network directly depends on the speed of the AVs.

To decide the speed of the AVs, the reliability, transmission rate, and latency of communication between AVs and the traffic control service running in the infrastructure are critical, in addition to the physical conditions of the roads, the density of vehicles, and the speed limit (v_l) imposed by the transportation authorities [3], [5], [23]. For instance, if the AVs have faster reaction times, they might be able to move faster and travel at closer distances with each other without compromising safety. This reaction time strongly depends on the reliability, transmission rate, and latency of the AV communication.

In this paper, we propose an approach that uses the speed values, computed by maximizing the throughput of a road network (from Lemma 1 in Section IV), as the *effective speed* (values) of AVs for route planning (in Section III). Specifically, these speed values are associated with RSs of a road network to form its effective speed map (ESM) to be used by the routing function. For computing the trip duration and planning the routes, as with current vehicle navigation systems, we assume that the ESM does not change for the time period that a target AV is routed, and this AV travels exactly at this effective speed.

B. γ -Rate Cell of a BS

In [11], BSs would control the AVs. For a BS, geometrically, we define its γ -rate cell to be the largest area surrounding the BS such that (1) the probability of having a downlink transmission rate¹ more than γ Mbps at any location within the area, is higher than a threshold of $1-\epsilon$, where ϵ is a very small number, and (2) for any two locations on the roads within this area, there exists a road path within the same area connecting them. Thus, each γ -rate cell is one contiguous region. Based on this definition, with rates $\gamma_1 < \gamma_2$, for a specific BS, its γ_1 -rate cell contains its γ_2 -rate cell. The two γ -rate cells of two adjacent BSs are connected if their overlapping area covers at least one common RI or one common RS. For example, owing to the channel hardening effect of massive MIMO [12], small-scale fading is mitigated and the magnitude of variations of transmission rates is small, so that the boundaries of γ -rate cells are stable over time even when ϵ goes to 0. Although it is not necessary to keep track of the exact boundary of a γ -rate cell, for AV navigation, it is good enough to keep track of all the RIs and RSs within the γ -rate cell of a BS.

In order to compute the γ -rate cells for the BSs, the probability that the transmission rate is above a given threshold γ should be recorded every few meters along the RSs. To obtain this probability corresponding to this distance, all the rate measurements within this interval should be reported through the BSs to the route planning function, together with the corresponding GPS locations.

III. COMMUNICATION-CONSTRAINED ROUTING (CCR)

The CCR problem can be stated as follows: find the shortest-time path from the source location to the destination location

¹AV applications can also have rate requirements for uplink transmissions. However, the methodology for solving the uplink CCR problem is the same. So, for simplicity, in this paper we consider only the downlink.

where the given minimum transmission rate can be sustained along the entire path at all times. In this section, we focus on routing one AV in a non-cooperative (selfish) manner. The AV is fully autonomous with collision avoidance, so that the time spent by this AV on waiting at RIs and yielding to pedestrians and other AVs is considered negligible [2], [5], [21].

A road network with deployed BSs over a given area, as depicted in Fig. 2(a), can be modeled as a graph $G_{\text{road}}(\mathcal{V}, \mathcal{E}, \mathcal{M})$ [16], where node set \mathcal{V} denotes the set of RIs, edge set \mathcal{E} represents the set of RSs connecting adjacent RIs, and \mathcal{M} is the set of BSs deployed in the given area. For BS $m \in \mathcal{M}$, G_{road}^m denotes the graph representing the part of the road network located within m 's γ -rate cell, as depicted in Fig. 2(b). For both G_{road} and G_{cell}^m , the weight of an edge (RS) is the travel time of an AV over this edge, which is computed as the length of this edge divided by the corresponding effective speed obtained from the ESM, which was discussed in Subsection II-A.

A. Two-Layered AV Routing Scheme

In [18], a road network was also modeled by a graph similar to G_{road} but without the component \mathcal{M} . To reduce routing complexity, [18] selected a subset of critical RIs to perform hierarchical routing. However, the performance of this approach strongly depends on the RIs selected and is usually suboptimal.

As in urban scenarios where the number of BSs is much smaller than the number of RIs (for instance, some cells have radii of as much as 1-2 km [27]), in contrast to [18], we propose to divide $G_{\text{road}}(\mathcal{V}, \mathcal{E}, \mathcal{M})$ into two layers to facilitate a two-layered routing scheme. The top layer is denoted by graph G_{BS} representing the connectivity among γ -rate-cells, and the bottom layer consists of all the graphs of γ -rate-cells (G_{cell}^m) of these BSs (as shown in Fig. 2(c)). Over these two layers, *inter*- γ -rate-cell routing and *intra*- γ -rate-cell routing are conducted in sequence followed by a process of dynamic programming to compute the shortest path between the source and destination locations. The optimality of the proposed scheme is demonstrated at the end of this subsection.

Specifically, in G_{BS} , there exists an edge between two γ -rate cells only when these two γ -rate cells are connected. Given that two γ -rate cells may be connected in the road network, via multiple common RIs and/or RSs, the exact travel time (i.e., weight) over a (top-layer) edge in G_{BS} between any two adjacent γ -rate cells is initially undefined. Therefore, for inter- γ -rate-cell routing, Breadth-First Search (BFS) is applied to find the set of all possible (top-layer) paths from the source γ -rate cell, through zero or more intermediate γ -rate cells, to the destination γ -rate cell². Let $\mathcal{P} = \{P_1, P_2, \dots, P_{|\mathcal{P}|}\}$ be the set of (top-layer) paths found, and $|P_i|$ be the number of γ -rate cells traveled in path P_i . For path P_i , $[\gamma C_1^i, \gamma C_2^i, \dots, \gamma C_{|P_i|}^i]$ denotes the sequence of γ -rate cells traveled (see the schematic diagram in Fig. 3), where γC_1^i and $\gamma C_{|P_i|}^i$ are the source and destination γ -rate cells in G_{BS} , respectively.

²Source (destination) γ -rate cell is defined as the γ -rate cell that contains the source (destination) location of the AV.

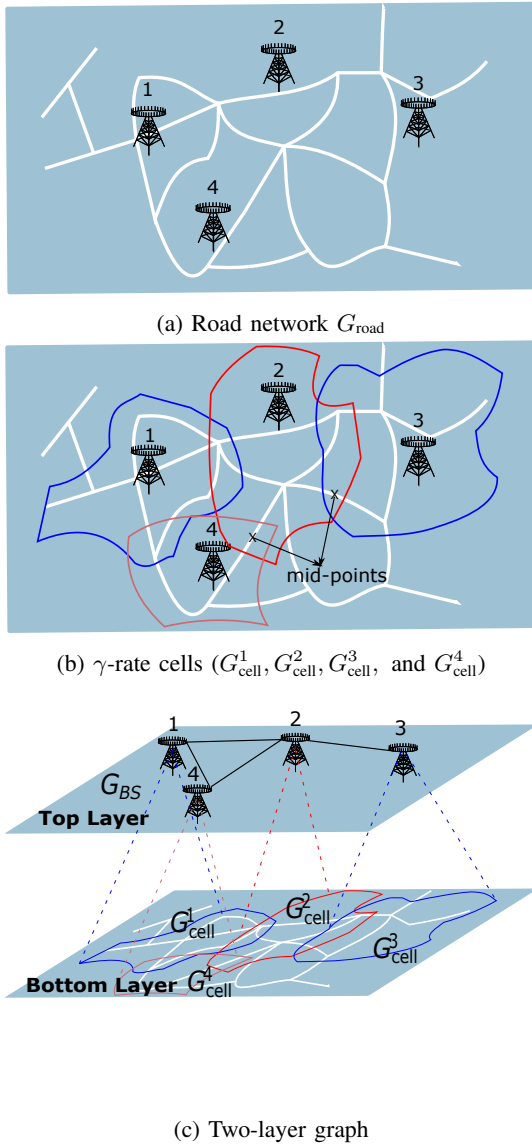


Figure 2: Transfer a road network into two layers

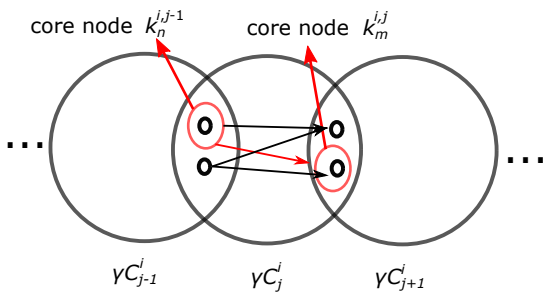


Figure 3: γ -rate cells and core nodes in path P_i . (The arrows in γC_j^i illustrate the proposed dynamic programming procedure.)

For path P_i , among the common RIs and RSs only between two adjacent γ -rate cells, the AV must pass through only one of them. We denote the common RIs between two adjacent γ -rate cells, as well as the mid-points (as indicated in Fig. 2(b)) of the common RSs that have no RIs on them, as *core nodes*. The set of core nodes between γC_j^i and γC_{j+1}^i is

denoted as $\mathcal{K}^{i,j} = \{k_1^{i,j}, k_2^{i,j}, \dots, k_{I_j}^{i,j}\}$. By using the Dijkstra shortest-path algorithm, the intra- γ -rate-cell routing computes the minimum travel time $T_{n,m}^{i,j}$ from core node $k_n^{i,j-1}$ (between γC_{j-1}^i and γC_j^i) to core node $k_m^{i,j}$ (between γC_j^i and γC_{j+1}^i), for all $k_n^{i,j-1}$ in $\mathcal{K}^{i,j-1}$ and $k_m^{i,j}$ in $\mathcal{K}^{i,j}$ on G_{cell}^j ³. In addition, let $T_{\text{opt}}^{i,j}$ denote the optimal travel time from the source location to core node $k_m^{i,j}$, through path i , and $T_0^{i,|P_i|}$ the optimal travel time from the source location to the destination location, through path i .

After inter- γ -rate-cell and intra- γ -rate-cell routing, dynamic programming is applied to compute $T_{\text{opt}}^{i,j}$, and eventually $T_0^{i,|P_i|}$. Overall the two-layered routing scheme is summarized as follows:

Step 1: Inter- γ -rate-cell routing. Find the set of all possible (top layer) paths on G_{BS} , \mathcal{P} , using BFS.

Step 2: Intra- γ -rate-cell routing. Use the Dijkstra shortest-path algorithm to compute the minimum travel time $T_{n,m}^{i,j}, \forall i, j, m, n$ and record the time with the corresponding path on the road network.

Step 3: Dynamic programming. $\forall i, j, m$, compute $T_{\text{opt}}^{i,j} = \min_n (T_n^{i,j-1} + T_{n,m}^{i,j})$. The shortest duration trip is then chosen to be $\min_i T_0^{i,|P_i|}$, with P_i^* being the chosen top-layer path. The bottom-layer road paths can be obtained from the recorded results in Step 2.

Remark 1: The necessary and sufficient condition for the two-layered routing scheme to have a solution is that the path set \mathcal{P} obtained in the inter- γ -rate-cell routing in Step 1 is not empty. If no result is obtained at Step 1, one option is to reduce the rate threshold γ until a path can be found.

Remark 2: The proposed scheme is optimal, as shown next. Each route from the source location to the destination location corresponds to one distinct top-layer path (P_i), and in Step 1, all such top-layer paths, \mathcal{P} , are found. For P_i , in Step 3, the shortest travel time $T_0^{i,|P_i|}$ is obtained using dynamic programming. Comparing $T_0^{i,|P_i|}$ for all i , all results are exhaustively examined, and the route with minimum $T_0^{i,|P_i|}$ is the optimal solution to the problem.

B. Simulation Results

We consider a Manhattan-like area as shown in Fig. 4, where $A = 11$ avenues and $S = 51$ streets divide the area into a grid topology of identical rectangles⁴. The corners of these rectangles are at the centers of the road intersections, the lengths and widths of which are $L = 250$ m and $W = 100$ m, respectively. $K = 21$ BSs are uniformly deployed in this area and all are equipped with $N_t = 128$ transmit antennas. Different from the realistic traffic patterns in Manhattan, we assume that all streets and avenues allow bidirectional traffic flows.

Given that there exists no other AV routing scheme subject to communication constraints, we compare the proposed two-layered AV routine scheme against two greedy routing

³Unlike G_{BS} , computing the shortest paths is possible because the edge weights of G_{cell}^j are defined to be the length of an RS divided by the effective speed from ESM.

⁴The use of a grid topology simplifies the greedy routing schemes used in the simulation.

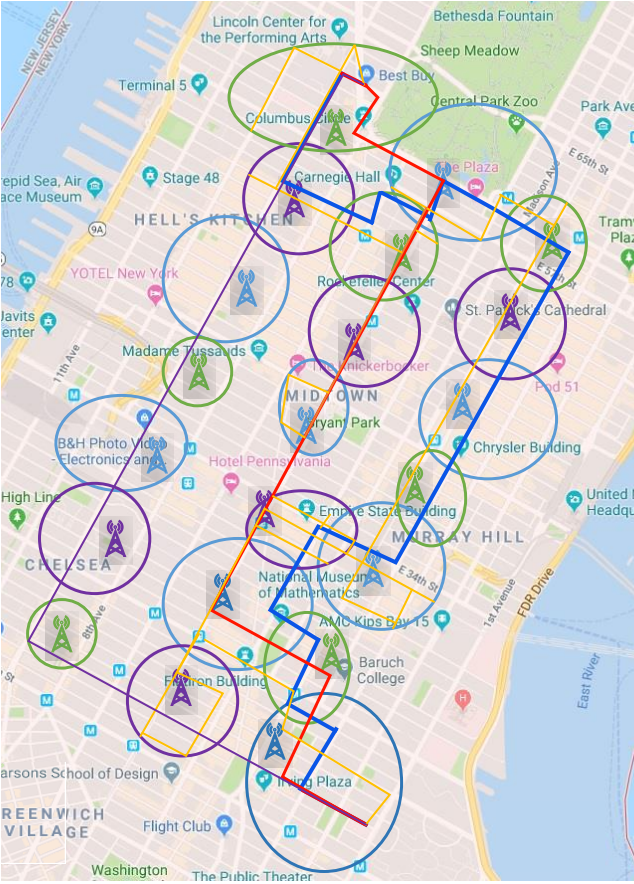


Figure 4: An example BS deployment in Manhattan and their γ -rate cells. The route in blue is computed by the “Two Layer” scheme; red by “Greedy w/o CC”; yellow by “Greedy s.t. CC”; purple by “Shortest Time”.

approaches performed locally by the AV, one without communication constraints and one with communication constraints.

1) *Greedy routing without communication constraints:* In the scenario of a grid topology, typically, when the destination is located, say, northwest of the source, at each RI, an AV would choose the next RS that is (close to) either north bound or west bound, but neither east nor south bound, in order to travel the shortest distance. Specifically, at each RI, for all available RSs that lead closer to the destination, one is randomly chosen as the next RS.

2) *Greedy routing subject to communication constraints:* In this scheme, while driving, the AV learns the availability of local RSs that could satisfy its communication constraints (from the information broadcast by BSs). Upon arriving at an RI, the AV will choose, among all the available local RSs that satisfy its communication constraints, the RS that leads closer to the destination. In the worst case, the AV has to backtrack (i.e., make a U-turn) to a previous RI to choose a different RS (that satisfies the communication constraints).

Using specific values of ESM and γ , Fig. 4 shows the routes computed by different routing schemes. The ‘circle’ around each BS represents its γ -rate cell. “Greedy w/o CC” and “Greedy s.t. CC” are the greedy methods introduced above, and “Shortest Time” chooses the shortest-time path using the

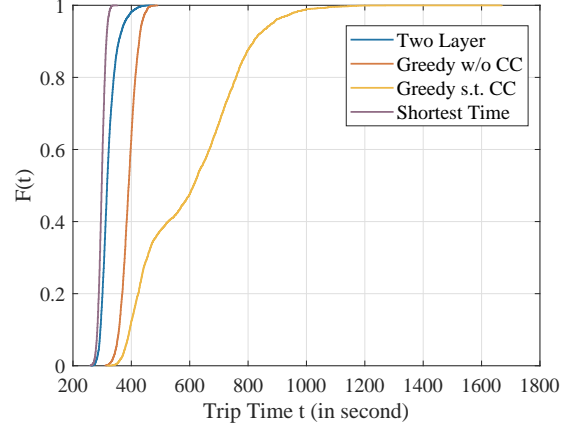


Figure 5: CDF of the trip duration (γ is 55 Mbps).

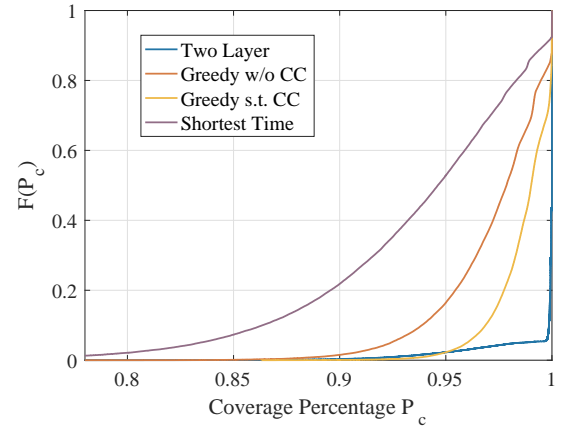


Figure 6: CDF of the percentage of trip duration covered by the required communication (γ is 55 Mbps).

Dijkstra algorithm without communication constraints. For the route computed by “Greedy s.t. CC”, although it is mostly covered by γ -rate cells, its track shows backtracking behavior.

In the simulation, we randomly generate the effective speeds for all RSs 10,000 times, from the set $\{10 \text{ m/s}, 20 \text{ m/s}, 30 \text{ m/s}\}$. These speeds are consistent with those used in [25]. The slot length in an LTE-A system, $\tau = 1 \text{ ms}$, is used as the channel measurement interval. Also, the Winner II path loss model for urban areas [28] is applied, and the transmission rates are computed using the method in [26]. Fig. 5 depicts the CDF of the resulting trip duration for the different routing schemes with $\gamma = 55 \text{ Mbps}$. The results show that the proposed two-layered routing scheme can achieve a trip duration close to the shortest-time routing while satisfying the communication requirements. Note that, due to the potential backtracking in “Greedy s.t. CC,” an upper bound on the maximum number of RSs traveled is set. When this limit is reached, to reach the destination, the AV switches from “Greedy s.t. CC” to “Greedy w/o CC”, as noticed by the “stepping” appearance of the yellow curve in Fig. 5.

Fig. 6 depicts the CDF of the percentage of the trip duration that the AV’s rate requirement is satisfied, P_c . The results show

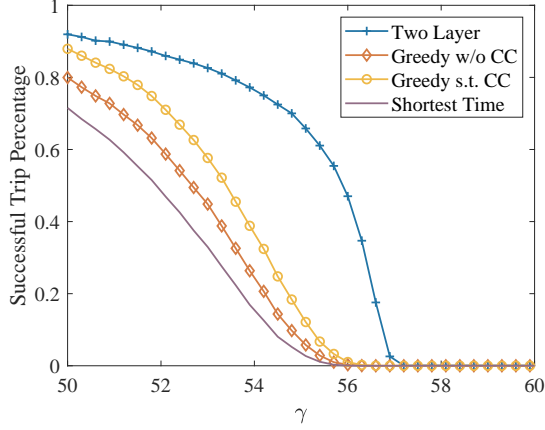


Figure 7: Successful trip percentage w.r.t γ .

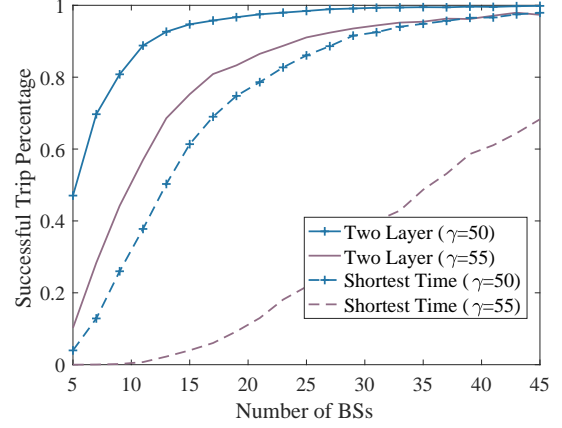


Figure 9: Successful trip percentage w.r.t the number of deployed BSs.

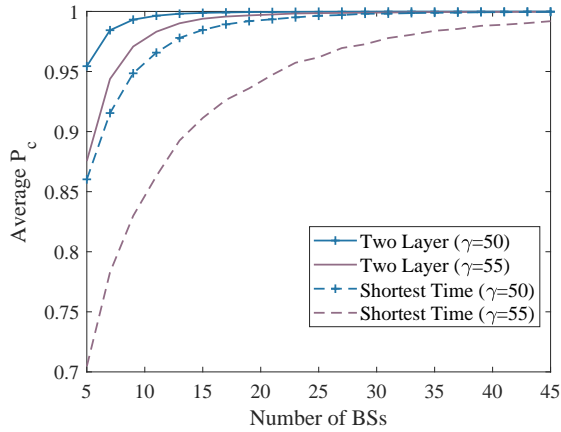


Figure 8: Percentage of the trip covered by the required communication w.r.t the number of deployed BSs.

that the proposed two-layered routing provides good communication coverage. In addition, because the “Shortest Time” scheme usually chooses RSs with higher effective speeds, the Doppler effect affects the transmission rates, resulting in worse coverage than “Greedy w/o CC.”

Furthermore, we compute the metric “successful trip percentage” defined as the probability that the target AV can find a route that satisfies the rate requirement along the entire trip. By varying the value of γ , the results, as shown in Fig. 7, show that, with increasing γ , it becomes more difficult to find a satisfactory route; however, the two-layered routing scheme always outperforms the other methods using this performance metric. In addition, we vary the number of BSs in the Manhattan area. The average P_c (average percentage of trip duration covered by the required transmission rates), as well as the successful trip percentage, are plotted in Figs. 8 and 9, respectively. These two figures show that, to achieve a specified communication requirement, with CCR of AV, fewer BSs are required for deployment, but with a longer trip duration.

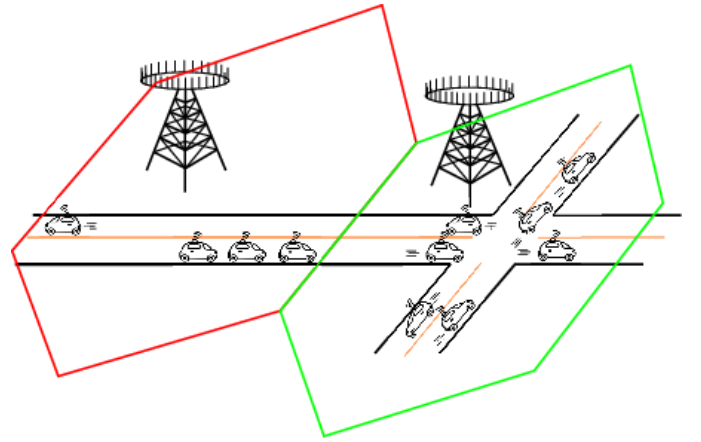


Figure 10: Scenario of traffic flow capacity mismatch across cells

IV. COMMUNICATION-CONSTRAINED TRAFFIC CONTROL (CCTC)

In the last section, we considered the routing of a single AV and ignored the impacts of other AVs, even though a BS can serve multiple AVs simultaneously. From the viewpoint of traffic control, maximizing the throughput capability of a road network is one primary goal of adopting AVs [21]. However, to achieve the optimal CCTC of maximizing the road-network throughput subject to communication constraints, several inter-related issues remain to be studied.

In this paper, we study two specific problems: (1) in one-cell scenarios, given the constrained communication resources, we investigate the number of AVs that can be served simultaneously by the BS as a new KPI for traffic control, and use the result to derive the optimal AV speed for maximizing the “sum traffic flow” into/out of the cell, and (2) in multi-cell scenarios, we study a traffic flow capacity mismatch problem across different cells along the same road, and propose a spectrum re-balancing solution to address the issue. Numerical results demonstrate that the one-cell and multi-cell solutions can be applied in sequence to maximize the road-network throughput.

A. Speed Optimization within Single Cell

As discussed in [3], to enable high LoA for AVs, certain minimum communication requirements of reliability, transmission rate, and latency, denoted by $\Gamma = [\mathcal{R}_0, \mathcal{G}_0, \mathcal{A}_0]$, must be satisfied for each AV⁵. We propose the following KPI, connecting Γ with AV traffic control, to indicate the traffic control performance of a single cell.

$\mathcal{N}_\Gamma^v(\mathcal{B})$, which denotes the largest number of AVs that a BS can control simultaneously subject to the communication requirements of Γ , where AVs are uniformly distributed within the BS's coverage area, all AVs move at speed v , and \mathcal{B} is the number of available frequency channels in this cell.

Note that $\mathcal{N}_\Gamma^v(\mathcal{B})$ monotonically increases with \mathcal{B} and decreases with v , given the same Γ . The decrease with speed results from the fact that more communication resources would need to be consumed for each AV traveling at higher speeds to satisfy Γ . Given the the same amount of available resources, fewer AVs could be controlled when traveling at higher speeds. For simplicity, we do not consider optimal channel allocation across channels; then, for identically distributed frequency channels within a cell, there exists a value \mathcal{B}_m such that the following linearity property holds.

$$\begin{aligned} \forall \mathcal{B}_1 + \mathcal{B}_2 < \mathcal{B}_m, \mathcal{N}_\Gamma^v(\mathcal{B}_1 + \mathcal{B}_2) &= \mathcal{N}_\Gamma^v(\mathcal{B}_1) + \mathcal{N}_\Gamma^v(\mathcal{B}_2) \\ \forall \mathcal{B} < \mathcal{B}_m, \mathcal{N}_\Gamma^v(\mathcal{B}) &= \mathcal{B} \mathcal{N}_\Gamma^v(1) \end{aligned}$$

When there is only one frequency channel, a BS can still control multiple AVs by using time-division multiplexing (TDM) or frequency-division multiplexing (FDM) to divide the channel into multiple subchannels, as well as by using MIMO. Here, we assume this linearity property always holds.

For simplicity, we assume that, within a cell, there is no lane merging and no dead ends, so that the numbers of lanes, \mathcal{L} , into and out of a cell are identical. (For instance, in Fig. 10, for the red cell, $\mathcal{L} = 2$; and for the green cell, $\mathcal{L} = 4$.) We define BS Coverage \mathcal{C} as the total surface area of the roads that the BS covers. The width of each lane is assumed to be \mathcal{W} ; then, the total length of all lanes in this cell is $\frac{\mathcal{C}}{\mathcal{W}}$.

Let $\mathcal{D}(v)$ denote the minimum distance between two AVs within the cell set by the transportation authority subject to effective speed v . For a steady flow of traffic, we consider that AVs are uniformly distributed in the BS's coverage area with speed v . Then, in theory, the distance between two consecutive AVs would be $\max\{\mathcal{D}(v), \frac{\mathcal{C}}{\mathcal{W}\mathcal{N}_\Gamma^v(\mathcal{B})}\}$. The result of dividing this distance by v becomes the average inter-arrival time between two consecutive AVs entering (or leaving) the cell. We define *cell sum traffic flow*, \mathcal{F}_m , to be the maximum number of AVs that is allowed to enter or leave a cell per minute. Then, by applying the equation on p. 319 in [33],

$$\mathcal{F}_m = \frac{\mathcal{L}v}{\max\{\mathcal{D}(v), \frac{\mathcal{C}}{\mathcal{W}\mathcal{N}_\Gamma^v(\mathcal{B})}\}}. \quad (1)$$

In practice, $\mathcal{D}(v)$ is small and can be eliminated from Eq. (1). Therefore, the average distance between consecutive AVs be-

comes $\frac{\mathcal{C}}{\mathcal{W}\mathcal{N}_\Gamma^v(\mathcal{B})}$. The result of dividing this average distance by v is the average inter-arrival time between two consecutive AVs entering or leaving the cell. Then,

$$\mathcal{F}_m = \frac{\mathcal{L}\mathcal{W}}{\mathcal{C}} \mathcal{N}_\Gamma^v(\mathcal{B})v. \quad (2)$$

Note that (2) holds even for non-steady-state flows, where the inter-arrival time between AVs entering a cell is not uniformly distributed. Then, for the one-cell case considered here, the following lemma shows that each cell has an optimal speed for maximizing the road-network throughput in that cell.

Lemma 1: Given the fixed amount of communication resources in a cell and the minimum communication requirements Γ for a specified LoA, there exists an optimal speed, and hence an optimal number of AVs, such that the road-network throughput in this cell is maximized when all AVs travel at this speed.

Proof. Given a fixed amount of communication resources in a cell, the relationship between $\mathcal{N}_\Gamma^v(\mathcal{B})$ and the AV speed v is a unique function, and $\mathcal{N}_\Gamma^v(\mathcal{B})$ monotonically decreases with v . $\mathcal{N}_\Gamma^v(\mathcal{B})$ peaks at $v = 0$. Also, there exists a speed threshold v_m such that, when all the AVs in the cell travel at a speed above this threshold, they become uncontrollable, i.e., $\mathcal{N}_\Gamma^v(\mathcal{B}) = 0$, when $v > v_m$. Therefore, $\mathcal{N}_\Gamma^v(\mathcal{B})v$ is upper bounded by $\mathcal{N}_\Gamma^0(\mathcal{B})v_m$. Because \mathcal{L} , \mathcal{W} , and \mathcal{C} are constants, there is an AV speed $v^* \leq v_m$ that maximizes $\mathcal{F}_m = \frac{\mathcal{L}\mathcal{W}}{\mathcal{C}} \mathcal{N}_\Gamma^v(\mathcal{B})v$ (\mathcal{F}_m^*), and $\mathcal{N}_\Gamma^{v^*}(\mathcal{B})$ is the corresponding optimal number of AVs. For this cell, this value of sum traffic flow \mathcal{F}_m^* is its maximum road-network throughput. \square

Lemma 1 only proves the existence of an optimal AV speed. To derive the optimal AV speed, it becomes necessary to obtain the unique function between $\mathcal{N}_\Gamma^v(\mathcal{B})$ and AV speed v . This function depends on the technology employed by the BS, which can be obtained by using either statistical methods or model-based methods. In Subsection IV-C, a model-based method is introduced for a Time Division Duplex (TDD) BS. Also note that the optimal AV speed can be used for constructing the ESM for the CCR problem from the previous section, and this speed could differ in different cells.

B. Spectrum Balancing across Multiple Cells

For reasons such as severe channel fading and/or a high number of AVs, it is possible that the available communication resources within a cell are being exhausted so that it will not be able to support the desired LoA when more AVs enter the cell. Fig. 10 depicts such a scenario where the green cell does not have enough communication resources to accommodate more AVs coming from the red cell, so AVs may need to back up at the cell boundary.

For a road crossing multiple cells, (communication constrained) traffic flow capacity mismatch between adjacent cells can lead to traffic congestion in a cell that supports less traffic flow. Among all the cells that a road travels across, we term the cell with the least amount of traffic flow capacity *bottleneck cell*. The overall traffic flow of a road is then constrained

⁵The higher the LoA, the more stringent the communication requirements Γ .

by the capacity of the bottleneck cell. Therefore, to avoid congestion, ideally, all the cells along a road should support the same traffic flow capacity. We provide Lemma 2, which shows that dynamic channel allocation across different cells provides a solution to mitigate the negative effects of the bottleneck cells. For instance, in current cellular systems, adjacent cells often use different frequencies to avoid inter-cell interference. Therefore, given the total number of channels \mathcal{B}_0 over an area, more channels should be assigned to the bottleneck cells to increase their allowed traffic flows, and hence the overall throughput of the road crossing multiple cells.

Consider the following scenario for Lemma 2. An area containing L_r one-way roads (a two-way road can be considered as two one-way roads) is fully covered by N_e hexagonal cells that do not overlap. Within this area, in total, there are \mathcal{B}_0 frequency channels, and within a cell, each channel can control the same number of AVs. No two cells in this area share the same channel. BS i assigns \mathcal{B}_{ij} frequency channels for the AVs on road j , such that the maximum traffic flow on this section of road j within cell i is \mathcal{F}_{ij} . $\sum_{i,j} \mathcal{B}_{ij} = \mathcal{B}_0$. We consider FDM and assume that each frequency channel can be divided into a large number of subchannels to control multiple AVs. Also, it is allowed to assign a fraction of the channels to a cell. The proof for TDM is similar.

Lemma 2: Given \mathcal{B}_0 frequency channels to control AVs over an area containing L_r one-way roads, a necessary and sufficient condition for deciding assignments \mathcal{B}_{ij} to achieve Pareto-optimal road throughput among the L_r roads in this area is that, for each road j , $\mathcal{F}_{i_1j} = \mathcal{F}_{i_2j}$ for all BSs i_1 and i_2 whose cells road j travels across.

Proof. Randomly assign all \mathcal{B}_0 channels across different roads and cells. Suppose road j crosses a sequence of cells $\mathcal{S}_j = \langle s_1, s_2 \cdots s_{I(j)} \rangle$ in turn. Then, the traffic flow capability on this road should be $\mathcal{F}_j = \min_{s_i \in \mathcal{S}_j} \mathcal{F}_{ij}$, which is constrained by the cell with the smallest \mathcal{F}_{ij} . After the initial assignment, repeatedly shift channels or their subchannels from the cell with highest \mathcal{F}_{ij} to the cell with lowest \mathcal{F}_{ij} , one subchannel at a time, until $\mathcal{F}_{i_1j} = \mathcal{F}_{i_2j}$ (if $\mathcal{F}_{i_1j} = \mathcal{F}_{i_2j}$ is not achievable due to the fact that the number of AVs has to be an integer, then at least $\mathcal{F}_{i_1j} \approx \mathcal{F}_{i_2j}$), $\forall s_{i_1}, s_{i_2} \in \mathcal{S}_j$. Repeat this process for all L_r roads in this area. With these adjustments, the road throughputs of L_r roads all become higher.

To further improve the throughput for road j , channels or subchannels need to be reassigned from the other roads. Because each channel can control the same number of AVs within a cell, if channels are switched between two roads, the number of channels for each of the roads stays the same, so that their allowed traffic flows stay the same. However, borrowing channels or subchannels is always at the cost of the other roads' throughputs. Thus, as long as $\mathcal{F}_{i_1j} = \mathcal{F}_{i_2j}$, $\forall s_{i_1}, s_{i_2} \in \mathcal{S}_j$, and $\forall j$, it is impossible to improve the throughput of a certain road without compromising another, and hence the throughputs for the L_r roads are Pareto-optimal. \square

Note that when frequency reuse is allowed across cells such that two cells not adjacent to each other may share the same spectrum, or when different subchannels can control different numbers of AVs, " $\mathcal{F}_{i_1j} = \mathcal{F}_{i_2j}$ for all BSs i_1 and i_2 " in

Lemma 2 is only a necessary condition for achieving Pareto-optimal road throughput.

Remark 3: From the two lemmas, it is possible that two adjacent cells may have different optimal speeds and different optimal distances between AVs. In practice, the movement control services running in the infrastructure would foresee such situations to gradually slow down or speed up AVs to avoid any abrupt change of speed when crossing cell boundaries along the road.

C. Illustrative Scenarios

1) *Derivation in one-cell scenarios:* We consider the speed optimization problem in a single-cell slotted TDD MIMO scenario, where the duration of each slot is T_{slot} . By periodically sending T_{pilot} -length (in sec) pilots to measure the channels, the BS can obtain *accurate channel information*; this information is critical for satisfying the downlink communication requirements Γ . In the downlink, the BS sends periodic messages to each AV at a repetition rate of λ_m , which means λ_m messages are sent per second. The duration of one message is T_m , in sec, which is an integer multiple of T_{slot} . Because of the linearity property discussed above in Subsection IV-A, we focus on one frequency channel in the analysis, and use TDM for sharing the channel.

Given accurate channel information, and using one frequency channel to send the T_m -length messages, L -user-MIMO technology is applied in the BS, such that, at every downlink time slot, Γ can be satisfied for a maximum of L AVs. Note that, in order for the repetitive message transmissions to be successful, the message inter-arrival time, $1/\lambda_m$, should be larger than the duration of one message, T_m ; then, $\lambda_m T_m < 1$.

To obtain channel information that is sufficient and accurate enough to satisfy the Γ requirements, each AV must periodically send pilots to measure its channel at a maximum time interval of $T_v \approx \frac{1}{\alpha f_D(v)}$, where $f_D(v)$ is the AV's Doppler frequency and α is a scaling factor larger than 1. $f_D(v) = \frac{v}{c} f_c$, where f_c is the carrier frequency and c is the speed of light. The " \approx " is because in practice T_v should be an integer multiple of T_{slot} . In the frequency domain, one channel contains multiple subchannels, and during the T_{pilot} -length measurement of one AV, this AV's pilots are sent over all these subchannels; however, since these pilots are sent at the same time during T_{pilot} , we focus only on the time domain in the analysis below. Note that, within one frequency channel, TDM is used for multiplexing; dividing the frequency channel into multiple subchannels is for OFDM rather than for FDM.

From the discussions in the two paragraphs above, in the time domain, the slots are occupied by the AVs, sending periodic channel measurement pilots in the uplink, in turn, as well as receiving messages from BSs periodically in the downlink, with at most L AVs sharing one downlink slot. Furthermore, within a time period T ($T \gg T_m$), each AV would require roughly T/T_v pilots, such that $N_\gamma^v(1)$ AVs would require $N_\gamma^v(1)(T/T_v)$ pilots, which take $\lceil \frac{N_\gamma^v(1)(T/T_v)T_{\text{pilot}}}{T_{\text{slot}}} \rceil$ slots. Also, for downlink message transmission using L -user

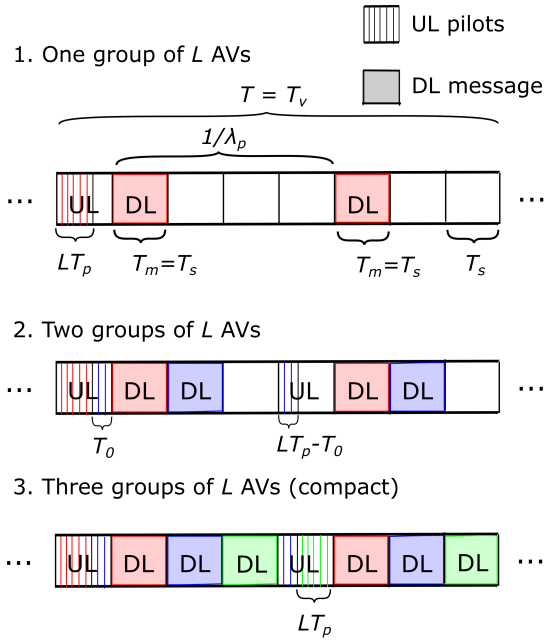


Figure 11: TDD MIMO downlink (DL) and uplink (UL) time slots filling-up during T . For the same color, there are two types of rectangular symbols with different patterns, respectively representing T_m -length downlink messages and uplink pilots for one group of L AVs. Red, blue, and green represent the first, second, and third group of L AVs.

MIMO, within a time period T , one group of L users would require $\lambda_m T$ T_m -length slots for sending messages, such that $N_\gamma^v(1)$ AVs would require $\lceil \frac{N_\gamma^v(1)}{L} \rceil \lambda_m T$ T_m -length slots. Part 1 of Fig. 11 shows an example of the slot utilization in a TDD MIMO scenario for one group of L AVs when $\lambda_m = 2/T_v = 2/T$ and $T_m = T_{\text{slot}}$, where, within duration T , there are $\lambda_m T = 2$ downlink messages and $LT/T_v = L$ uplink pilots.

Compared with former generations of cellular systems, in 5G, more flexible TDM is allowed, as shown in Fig. 2 in [35]. Specifically, adjacent slots can be independently used for uplink and downlink transmissions. With such flexibility, the numbers of uplink slots and downlink slots can be arbitrarily specified. As shown in Fig. 11, with the increase in the number of AVs, eventually, it reaches a point where the time slots in T are compactly filled by pilots and messages of $3L$ AVs, and no additional AVs can be accommodated. Thus, with flexible TDM in 5G, the sum lengths of all uplink pilots and downlink messages (both in sec) within duration of T , can occupy a duration close to T .

For the TDD MIMO scenario in this subsection, let

$$\lceil \frac{N_\gamma^v(1)(T/T_v)T_{\text{pilot}}}{T_{\text{slot}}} \rceil T_{\text{slot}} + \lceil \frac{N_\gamma^v(1)}{L} \rceil (\lambda_m T) T_m \leq T \quad (3)$$

When T_{slot} is small, $\lceil \frac{N_\gamma^v(1)(T/T_v)T_{\text{pilot}}}{T_{\text{slot}}} \rceil T_{\text{slot}} \approx N_\gamma^v(1)(T/T_v)T_{\text{pilot}}$. Then, we let

$$N_\gamma^v(1)(T_{\text{pilot}}/T_v) + \lceil \frac{N_\gamma^v(1)}{L} \rceil \lambda_m T_m \leq 1 \quad (4)$$

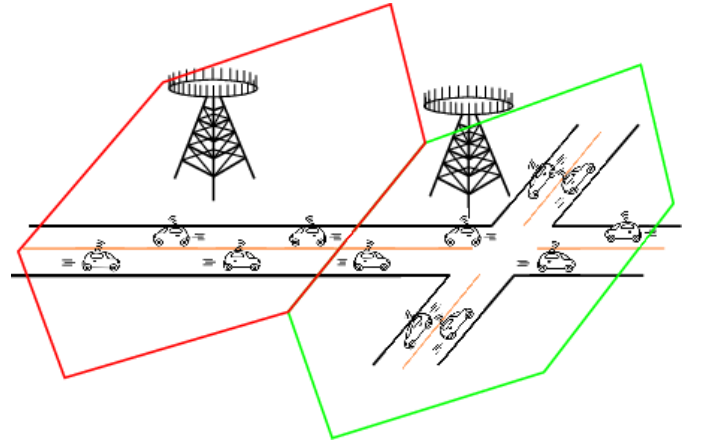


Figure 12: Matched traffic flow across cells

Also, when $N_\gamma^v(1) = iL$, $\lceil \frac{N_\gamma^v(1)}{L} \rceil = \frac{N_\gamma^v(1)}{L}$, $\forall i \in \mathbb{N}_0$, where \mathbb{N}_0 is the set of non-negative integers. And when $jL < N_\gamma^v(1) \leq (j+1)L$, $\lceil \frac{N_\gamma^v(1)}{L} \rceil = j+1$, $\forall j \in \mathbb{N}_0$. Because $N_\gamma^v(1)$ is an integer, the theoretical maximum number of AVs in the cell, from the viewpoint of filling up time slots, is

$$N_\gamma^v(1) = \begin{cases} \lfloor \frac{1}{T_{\text{pilot}}/T_v + \frac{1}{L}\lambda_m T_m} \rfloor, & \text{for } N_\gamma^v(1) = iL \\ \lfloor \frac{1 - (j+1)\lambda_m T_m T_v}{T_{\text{pilot}}} \rfloor, & \text{for } jL < N_\gamma^v(1) \\ & \leq (j+1)L \end{cases} \quad (5)$$

Given (5), it can be proved that \mathcal{F}_m in (2) reaches its peak when $N_\gamma^v(1) = \frac{1}{T_{\text{pilot}}/T_v + \frac{1}{L}\lambda_m T_m} = L$; solving this gives

$v = \frac{c(1 - \lambda_m T_m)}{\alpha f_c T_{\text{pilot}} L}$. Therefore, the best strategy to maximize \mathcal{F}_m is to choose speed

$$v^* = \min\{v_l, \frac{c(1 - \lambda_m T_m)}{\alpha f_c T_{\text{pilot}} L}\}, \quad (6)$$

where v_l is the speed limit imposed by the transport authority. The corresponding theoretical maximum cell sum traffic flow is

$$\mathcal{F}_m^* = \frac{\mathcal{LW}}{C} N_\gamma^{v^*}(1) v^* = \frac{\mathcal{LW}}{C} \lfloor \frac{1}{T_{\text{pilot}}/T_{v^*} + \frac{1}{L}\lambda_m T_m} \rfloor v^* \quad (7)$$

2) *Example in a two-cell scenario:* To demonstrate Lemma 2, we consider a frequency channel allocation problem using the two-cell scenario. As shown in Fig. 12, there are two horizontal lanes in the red cell, and two horizontal lanes and two vertical lanes in the green cell. In the red (green) cell, the AVs move at identical speed and the distances between two adjacent AVs on each lane are identical, thus the lanes' corresponding AV throughputs in the red (green) cell are also identical. This means, for the red cell, the cell sum traffic flow is the same as the sum traffic flow of the cell's horizontal lanes;

and for the green cell, the former is twice the latter. Then, to achieve Pareto-optimal road-network throughput, intuitively, the number of frequency channels assigned to the green cell, \mathcal{B}_g , should be larger than that of the red, \mathcal{B}_r , to make the traffic flows on the horizontal road smooth. $\mathcal{B}_0 = \mathcal{B}_g + \mathcal{B}_r$.

Denote the tuple of the number of lanes, the cell coverage, the optimal AV speed, and the maximum number of AVs, for the green cell, as $(\mathcal{L}_g = 4, \mathcal{C}_g, v_g, \mathcal{N}_{g,\Gamma}^{v_g}(\mathcal{B}_g))$, and for the red cell as $(\mathcal{L}_r = 2, \mathcal{C}_r, v_r, \mathcal{N}_{r,\Gamma}^{v_r}(\mathcal{B}_r))$. Then, using Lemma 2, the sum traffic flow of the red cell's horizontal lanes is the same as that of the green cell', and the cell sum traffic flow of the green cell is twice that of the red

$$\frac{\mathcal{L}_g \mathcal{W}}{\mathcal{C}_g} \mathcal{N}_{g,\Gamma}^{v_g}(\mathcal{B}_g) v_g = 2 \frac{\mathcal{L}_r \mathcal{W}}{\mathcal{C}_r} \mathcal{N}_{r,\Gamma}^{v_r}(\mathcal{B}_r) v_r \quad (8)$$

For the rest of this section, we consider the special case when the geometries of the two cells are identical; specifically, $\mathcal{C}_g = 2\mathcal{C}_r$, $v_g = v_r$, and the two functions $\mathcal{N}_{g,\Gamma}^v(\mathcal{B}) = \mathcal{N}_{r,\Gamma}^v(\mathcal{B})$. Then, solving Eq. (8), the optimal number of allocated channels are $\mathcal{B}_g = 2\mathcal{B}_r = 2/3\mathcal{B}_0$. Compared with equal channel allocation $\mathcal{B}_r = \mathcal{B}_g = 1/2\mathcal{B}_0$, it can be verified that $\mathcal{B}_g = 2\mathcal{B}_r = 2/3\mathcal{B}_0$ brings an additional road-network throughput gain of 33.3% for this two-cell scenario.

3) *Numerical results:* Here, we use the one-cell scenario derivations in this subsection for both the red and green cells in Fig. 12. Let $\mathcal{W} = 3$ m and the BS coverage of the red cell $\mathcal{C}_r = 12,000$ m². $L = 10$. Since 5G allows mini-slot of duration 0.1 ms, for the length of uplink channel measurement pilot, we let $T_{\text{pilot}} = 0.5$ ms [35]. According to [3], [30], $\lambda_m \in [10, 100]$ Hz and $T_m \in [1, 100]$ ms. For simplicity, it is assumed that v_l is large enough to be neglected. Then, for a total of $\mathcal{B}_0 = 10$ frequency channels, the theoretical road-network throughputs for the scenario in Fig. 12 are plotted in Figs. 13 and 14, for different values of α , f_c , $\lambda_m T_m$, and different traffic control approaches. ‘‘Naive Approach’’ is the benchmark when neither of the optimizations in Lemma 1 and 2 are used; specifically, in both cells, AVs move at a suboptimal speed $v^*/2$ and \mathcal{B}_0 is equally allocated to the two cells. In contrast, ‘‘Use Lemma 1’’ uses optimal speed v^* and ‘‘Use Lemma 1 & 2’’ utilizes the optimization results of both Lemma 1 and 2.

From Fig. 13, we can see that, the theoretical road-network throughput decreases with f_c and α . It means that the throughput decreases with the required amount of channel measurements (the increase of channel measurements is caused either by faster-varying channel as indicated by f_c , or by more stringent channel accuracy requirement as indicated by α). From Fig. 14, we can see that the theoretical road-network throughput decreases with $\lambda_m T_m$. It means that this throughput decreases with the amount of downlink messages required by AVs (the increase of downlink messages is caused either by being sent more frequently as indicated by λ_m or by longer messages as indicated by T_m). The unsmoothness of ‘‘Naive Approach’’ curves in Fig. 14 is due to the floor operator in Eq. (5).

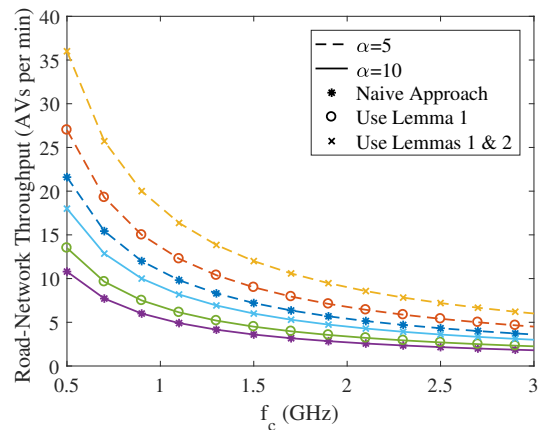


Figure 13: Road-network throughput w.r.t carrier frequency f_c ($\lambda_m T_m = 0.25$).

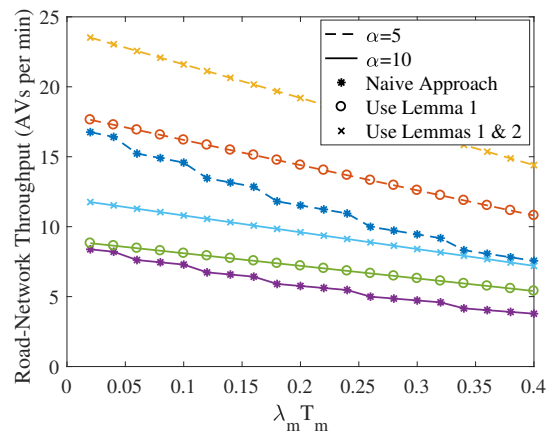


Figure 14: Road-network throughput w.r.t $\lambda_m T_m$ ($f_c = 1$ GHz).

V. CONCLUSION AND FUTURE WORK

In this paper, the problems of CCR and CCTC are motivated and investigated. For CCR, a two-layered routing scheme, including both inter- γ -rate-cell and intra- γ -rate-cell routing, is proposed, and its performance is compared with two greedy solutions. For CCTC, optimal effective speed and optimal frequency channel allocation across adjacent cells are derived to maximize theoretical road-network throughput within each cell and Pareto-optimal road-network throughputs across multiple cells.

The CCR and CCTC problems have variations that remain to be formulated and resolved. For instance, in CCR, except rate requirement, AV applications may have various communication QoS and edge computing requirements [36]. The co-existence of AVs and other cellular users can change the communication resources in each cell available for AVs, in which case the graph of road network is time-varying [31]-[32]. For CCTC, except maximizing road-network throughput, there are other goals in AV traffic control, for instance, minimizing trip duration and increasing energy efficiency. Also, in practice, more advanced technologies, like optimal subchannel

allocation for broadband communication and the collaboration of multiple BSs, can be used to increase the number of AVs one BS (or BSs) control simultaneously. In addition, some practical factors might be involved for more accurate modeling in CCR and CCTC, for instance, acceleration (deceleration) and group behavior in AV movement control; different AVs may have heterogeneous communication requirements and LoAs, and different BSs may provide heterogeneous communication capabilities; and the road network may be complex involving road signs, lane merging, roundabout, and parking capability.

REFERENCES

- [1] J. Andrews, T. Humphrey, C. Bhat, R. Heath, L. Narula, C. Choi, and J. Li "Evaluation of Routing Protocols for Vehicular Ad hoc Networks (VANETs) in Connected Transportation Systems," *Report No., D-STOP2017/135*, D-STOP at the University of Texas at Austin, Feb. 2018.
- [2] S. A. Bagloee, M. Tavana, M. Asadi, and T. Oliver, "Autonomous vehicles: challenges, opportunities, and future implications for transportation policies," *Journal of Modern Transportation*, vol. 24, no. 4, pp. 284-302, Dec. 2016.
- [3] 3GPP TR 22.886 V16.2.0 (2018-12). Study on enhancement of 3GPP support for 5G V2X services.
- [4] V. Shivaldova, A. Winkelbauer, and C. Mecklenbrauker, "Vehicular link performance: from real-world experiments to reliability models and performance analysis," *IEEE Veh. Technol. Mag.*, vol. 8, no. 4, pp. 35-44, Dec. 2013.
- [5] D. R. Stephens, T. J. Timcho, R. A. Klein, J. L. Schroeder, "Vehicle-to-infrastructure (V2I) safety applications concept of operations," *Report No. FHWA-JPO-13-060*, FHWA Office of Safety Research and Development, Mar. 2013.
- [6] 3GPP TS 22.186 V15.3.0 (2018-06) 13 Release. Service requirements for enhanced V2X scenarios.
- [7] IEEE 5G and beyond technology roadmap white paper, by IEEE 5G Initiative, Oct. 2017.
- [8] J. Gozalvez, M. Sepulcre, and R. Bauza, "IEEE 802.11p vehicle to infrastructure communications in urban environments," *IEEE Commun. Mag.*, vol. 50, no. 5, pp. 176-183, May 2012.
- [9] S. Temel, M. C. Vuran, and R. K. Faller, "A primer on vehicle-to-barrier communications: Effects of roadside barriers, encroachment, and vehicle braking," in *Proc. of 2016 IEEE 84th Vehicular Technology Conference*, Fall, 2016.
- [10] F. Rossi, R. Zhang, Y. Hindy, and M. Pavone, "Routing autonomous vehicles in congested transportation networks: structural properties and coordination algorithms," *Autonomous Robots*, Vol. 42, no. 7, pp. 1427-1442, Oct. 2018.
- [11] Cellular V2X Communications towards 5G. 5G Americas White Paper. Mar. 2018.
- [12] T. L. Marzetta, "Noncooperative cellular wireless with unlimited number of base station antennas," *IEEE Trans. Wireless Commun.*, vol. 9, no. 11, pp. 3590-600, Nov. 2010.
- [13] E. G. Larsson, O. Edfors, F. Tufvesson, and T. L. Marzetta, "Massive MIMO for next generation wireless system," *IEEE Commun. Mag.*, vol. 52, no. 2, pp. 186-195, Feb. 2014.
- [14] 3GPP TS 22.261 V16.60 (2018-12). Service requirements for next generation new services and markets.
- [15] J. J. Q. Yu and A. Y. S. Lam, "Autonomous vehicle logistic system: joint routing and charging strategy," *IEEE Trans. Intelligent Trans. Sys.*, vol. 19, no. 7, Jul. 2018.
- [16] T. Wang, C. G. Cassandras, and S. Pourazarm, "Energy-aware vehicle routing in networks with charging nodes," in *Proc. of 19th world congress the international federation of automatic control*, Cape Town, Aug. 2014.
- [17] M. M. Nejad, L. Mashayekhy, D. Grosu, and R. B. Chinnam, "Optimal routing for plug-in hybrid electric vehicles," *Transportation Science*, vol. 51, no. 4, pp. 1031-1386, Nov., 2017.
- [18] Q. Li, Z. Zeng, and B. Yang, "Hierarchical model of road network for route planning in vehicle navigation systems," *IEEE Trans. Intelligent Trans. Sys.*, vol. 1, no. 2, pp. 20-24, Sept. 2009.
- [19] P. Sanders and D. Schultes, "Highway hierarchies hasten exact shortest path queries," in *Proc. of the 13th European Symposium on Algorithms, ESA05*, pp. 568-579, 2005.
- [20] P. Sanders and D. Schultes, "Engineering fast route planning algorithms," in *Proc. of Experimental Algorithms WEA 2007*, vol. 4525, Springer, Berlin, Heidelberg, 2007.
- [21] S. Boyles and M. Levin, "Improved traffic operations through real-time data collection and control," *Report No., D-STOP2016/108*, D-STOP at the University of Texas at Austin, Feb. 2018.
- [22] V. Milanés, J. Villagra, J. Godoy, J. Simo, J. Perez, and E. Onieva, "An intelligent V2I-based traffic management system," *IEEE Trans. Intelligent Trans. Sys.*, vol. 13, no. 1, pp. 49-58, Mar. 2012.
- [23] P. Zachariou, J. James, C. Hammond, B. Naveen, and R. Mayson, "Speeding effects on hazard perception and reaction time," *Report No. 243*, High Road Automotive Research, Feb. 2011.
- [24] L. T. Tan and R. Q. Hu, "Mobility-aware edge caching and computing in vehicle networks: a deep reinforcement learning," *IEEE Trans. Veh. Tech.*, vol. 67, no. 11, pp. 10190-10203, Nov. 2018.
- [25] 3GPP TR 36.885 V14.0.0 (2016-06). Study on LTE-based V2X services.
- [26] A. K. Papazafeiropoulos, "Impact of general channel aging conditions on the downlink performance of massive MIMO," *IEEE Trans. Veh. Technol.*, vol. 66, no. 2, pp. 1428-1442, Feb. 2017.
- [27] A. Goldsmith, *Wireless Communications*. Cambridge Univ. Press, 2005.
- [28] IST-4-027756 WINNER II D1.1.2 V1.2. WINNER II Channel Models.
- [29] H. Ji, S. Park, J. Yeo, Y. Kim, J. Lee, and B. Shim, "Ultra-reliable and low-latency communications in 5G downlink: physical layer aspects," *IEEE Wireless Commun.*, vol. 25, no. 3, pp. 124-130, Jun. 2018.
- [30] X. Ge, "Ultra-reliable low-latency communications in autonomous vehicular networks," *IEEE Trans. Veh. Tech.*, vol. 68, no. 5, pp. 5005 - 5016, Mar. 2019.
- [31] W. Huang and L. Ding, "The shortest path problem on a fuzzy time-dependent network," *IEEE Trans. Commun.*, vol. 60, no. 11, pp. 3376-3385, Sept. 2012.
- [32] W. Huang and J. Wang, "The shortest path problem on a time-dependent network with mixed uncertainty of randomness and fuzziness," *IEEE Trans. Intel. Trans. Sys.*, vol. 17, no. 11, pp. 3194-3204, Apr. 2016.
- [33] B. Friedrich, *The Effect of Autonomous Vehicles on Traffic*, Springer, Berlin, Heidelberg, 2016.
- [34] S. Vishwanath, N. Jindal, and A. Goldsmith, "Duality, achievable rates and sum rate capacity of Gaussian MIMO broadcast channels," *IEEE Trans. Inf. Theory*, vol. 49, pp. 2658-2668, Oct. 2003.
- [35] S.-Y. Lien, S.-L. Shieh, Y. Huang, B. Su, Y.-L. Hsu, and H.-Y. Wei, "5G New Radio: waveform, frame structure, multiple access, and initial access," *IEEE Commun. Mag.*, vol. 55, no. 6, pp. 64-71, Jun. 2017.
- [36] VR and AR Pushing Connectivity Limits White Paper. Qualcomm, Oct. 2018.